SCISPACE
formerly Typeset

Open access • Journal Article • DOI:10.1209/EPL/I2006-10168-7

Linear analysis of the cylinder wake mean flow — Source link

Dwight Barkley

Institutions: University of Warwick

Published on: 01 Sep 2006 - EPL (EDP Sciences)

Topics: Strouhal number, Vortex shedding, Reynolds number, Mean flow and Laminar flow

Related papers:

- Global stability of base and mean flows : a general approach and its applications to cylinder and open cavity flows
- On the frequency selection of finite-amplitude vortex shedding in the cylinder wake
- Structural sensitivity of the first instability of the cylinder wake
- GLOBAL INSTABILITIES IN SPATIALLY DEVELOPING FLOWS: Non-Normality and Nonlinearity
- A hierarchy of low-dimensional models for the transient and post-transient cylinder wake

Share this paper:

View more about this paper here: https://typeset.io/papers/linear-analysis-of-the-cylinder-wake-mean-flow-4b94lbbo3f

EUROPHYSICS LETTERS 1 September 2006

Europhys. Lett., **75** (5), pp. 750–756 (2006)
DOI: 10.1209/epl/i2006-10168-7

Linear analysis of the cylinder wake mean flow

D. Barkley(*)
Mathematics Institute, University of Warwick - Coventry, CV4 7AL, UK

received 27 March 2006; accepted in final form 7 July 2006
published online 26 July 2006

PACS. 47.20.Ft – Instability of shear flows (*e.g.*, Kelvin-Helmholtz).
PACS. 47.20.Ky – Nonlinearity, bifurcation, and symmetry breaking.

Abstract. – A highly accurate 2D linear stability analysis is performed on the mean flow of laminar vortex shedding from a circular cylinder for Reynolds numbers between 46 and 180. Consistent with past studies of mean profiles, the analysis shows that the eigenfrequency of the mean flow tracks almost exactly the Strouhal number of vortex shedding. The linear growth rate reveals that the wake mean flow is a marginally stable state over the whole range of Reynolds numbers for stable 2D vortex shedding. This is contrasted with 2D stability analysis about the unstable steady base flow. The relevance to nonlinear saturation and frequency selection are discussed.

Introduction. – Fluid flow past a circular cylinder has long been a prototype for bluff-body wake flows. The flow configuration is governed by a single non-dimensional parameter, the Reynolds number $Re = U_\infty d/\nu$, where ν is the kinematic viscosity of the fluid which is moving with free-stream speed U_∞ and d is the cylinder diameter. For values of Re below a critical value $Re_c \simeq 46$, the flow is asymptotically steady and two-dimensional. (See fig. 1(a) discussed in detail below.) At $Re = Re_c$ the steady flow becomes unstable through a Hopf bifurcation leading to the oscillating Bénard-von Karman vortex street [1–5]. (See fig. 1(b).) The flow is asymptotically time-periodic and two-dimensional for Re up to approximately 188, where the flow becomes three-dimensional [6]. This oscillatory flow is one of the most famous and well-studied flows in fluid mechanics.

A substantial body of work, both experimental and theoretical, has been devoted to understanding the vortex shedding frequency and spatial structure of the cylinder wake and other wake flows, *e.g.* [3–21]. Over the years a theory of spatially developping flows has advanced to the point of addressing fully nonlinear structures in wakes [17,18]. Of particular interest here is recent work by Pier [18] in which, among other things, he finds that the time average of the oscillating wake (the mean flow) provides the best profile from which to predict the shedding frequency. There are many other studies, *e.g.* [7, 8, 16, 21], in which averaged wake profiles have been used to determine shedding frequency. Another important way in which wake mean flows have received attention is in the work of Wesfreid *et al.* [13,15] and Noack *et al.* [19,20] on modification of the mean flow due to the oscillating wake and on the subsequent nonlinear saturation via interaction with the mean flow. These ideas trace back to the early work of

(*) E-mail: barkley@maths.warwick.ac.uk

© EDP Sciences
Article published by EDP Sciences and available at http://www.edpsciences.org/epl or http://dx.doi.org/10.1209/epl/i2006-10168-7

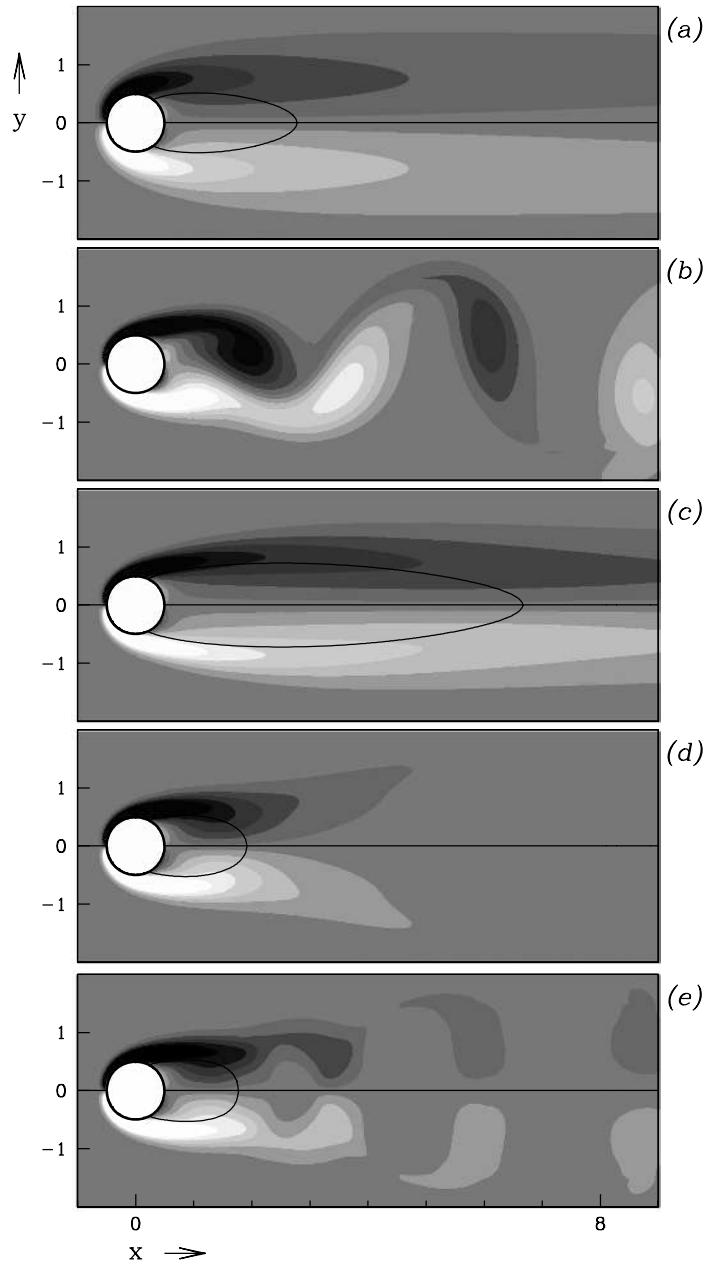

Fig. 1 – Flow visualisations illustrating the different types of states considered in this paper. Vorticity $\omega = \partial v/\partial x - \partial u/\partial y$ is plotted in greyscale with $\omega \leq -4$ black and $\omega \geq 4$ white. For the steady cases separating streamlines are plotted. Only a small portion of the full computational domain is shown. (a) $Re = 40$, below the onset of vortex shedding. The flow is steady, stable and reflection symmetric in y. In (b)-(d) $Re = 100$, well above the onset of vortex shedding. (b) A snapshot of the vortex shedding state. (c) The steady, but unstable base flow. The flow is reflection-symmetric in y and evolves continuously from (a) as a function of Re. (d) The mean flow over one shedding period. (e) Approximation to the mean flow obtained from the single snapshot in (b).

Stuart on nonlinear stability theory [22]. Noack *et al.* [19] present an appealing three-variable model capturing many aspects of 2D cylinder wake dynamics. The model suggests that the amplitude of the oscillating wake saturates precisely when the mean flow is marginally stable. This is similar in certain respects to the marginal stability criterion of Malkus [23] for fully developed turbulent flows.

Motivated by these studies of wake mean flows, we have undertaken a fully 2D linear stability analysis of the mean flow for the cylinder wake. A highly accurate numerical approach resolves the wake, and hence the mean flow, throughout a 2D domain and provides eigenvalues and 2D eigenmodes. Significantly we determine not only the linear eigenfrequency, but also the linear growth rates for general 2D (global) perturbations to the mean flow.

Simulations. – The flow is governed by the 2D incompressible Navier-Stokes equations

$$\frac{\partial \boldsymbol{u}}{\partial t} + (\boldsymbol{u}\cdot\boldsymbol{\nabla})\boldsymbol{u} \;=\; -\nabla p + \frac{1}{Re}\boldsymbol{\nabla}^2\boldsymbol{u}, \tag{1a}$$

$$\boldsymbol{\nabla}\cdot\boldsymbol{u} \;=\; 0, \tag{1b}$$

where $\boldsymbol{u}(x,y,t) = (u(x,y,t), v(x,y,t))$ is the velocity, $p(x,y,t)$ is the static pressure, and the density is one. These equations are nondimensionalised by the cylinder diameter d and the speed U_∞ of the free-stream flow, which is taken to be in the $+\hat{x}$ direction.

Equations (1) are numerically solved on a large 2D computational domain using a highly-accurate spectral-element discretisation with second-order differences in time. Details are given in refs. [6,24]. The cylinder is centred at the origin. The lateral dimensions of the domain are: $-16 \le x \le 25$ and $|y| \le 22$. No-slip conditions are imposed on the cylinder. Uniform flow, $(u,v) = (U_\infty = 1, 0)$, is imposed upstream and on the lateral sides, and an outflow boundary condition is imposed at the downstream end of the domain. This computational domain captures very accurately the wake flow over the range of Re of interest here [6].

Figure 1(a) shows the flow at $Re = 40$, below the onset of vortex shedding. The flow is steady and satisfies reflection symmetry about the centreline $y = 0$:

$$(u(x,y), v(x,y)) = (u(x,-y), -v(x,-y))\,. \tag{2}$$

Hence, as can be seen, the vorticity satisfies $\omega(x,y) = -\omega(x,-y)$. This flow is stable and starting from any initial condition, solutions $\boldsymbol{u}(x,y,t)$ to eqs. (1) converge to it as $t \to \infty$.

For $Re > Re_c$ the instantaneous reflection symmetry spontaneously breaks and the flow oscillates, shedding opposite sign vorticity downstream. Figure 1(b) shows a snapshot of the classic vortex street at $Re = 100$. This time-periodic flow has the spatio-temporal symmetry

$$(u(x,y,t), v(x,y,t)) = (u(x,-y,t+T/2), -v(x,-y,t+T/2))\,, \tag{3}$$

where T is the shedding period. The vorticity obeys $\omega(x,y,t) = -\omega(x,-y,t+T/2)$, so that one half a shedding cycle later the vorticity field in fig. 1(b) would be flipped about $y = 0$ with greyscale contours interchanged (*e.g.* white with black).

The Strouhal number St —the nondimensional shedding frequency $1/T$— is plotted in fig. 2(a) as a function of Re. The curve is a fit to data taken at discrete values of Re. At the numerical resolution of this study the curve is extremely accurate. As stated at the outset, a substantial amount of research has been devoted to understanding the relationship between St and Re seen in fig. 2(a).

Base flows. – We use $\boldsymbol{u}_b$ to denote base flows. These are time-independent solutions to eqs. (1). Below Re_c, *e.g.* fig. 1(a), the base flow is the unique stable state. Above Re_c, the

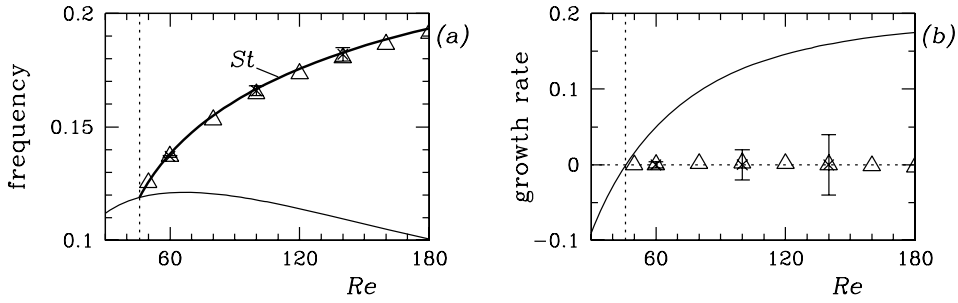

Fig. 2 – (a) Frequencies and (b) growth rates as a function of Reynolds number. In (a) the bold curve labelled St is the Strouhal number —the nondimensional vortex shedding frequency. All other results in (a) and (b) are from linear stability computation. Thin curves are for the base flow $\boldsymbol{u}_b$. Triangles are for the mean flow $\bar{\boldsymbol{u}}$. Crosses are for the two-point approximation to mean flow $\boldsymbol{u}_h$ with error bars indicating the spread of values depending on the reference time t_0. Vertical dashed lines indicate Re_c.

base flow still exists, but is unstable. Figure 1(c) shows $\boldsymbol{u}_b$ at $Re = 100$. The flow exhibits a very long recirculation region behind the cylinder. While this base flow is unstable, it can be obtained by direct numerical simulations by restricting to the subspace of symmetric solutions for which eq. (2) holds. This restriction can be accomplished in practice by imposing the constraint $v(x, y = 0) = 0$ in simulations of eqs. (1).

The linear stability of the base flow is determined from the evolution of infinitesimal perturbations $\epsilon\tilde{\boldsymbol{u}}$ to $\boldsymbol{u}_b$. Specifically, letting $\boldsymbol{u}(x, y, t) = \boldsymbol{u}_b(x, y)+\epsilon\tilde{\boldsymbol{u}}(x, y) \exp[\lambda t]$, substituting this into eqs. (1) and keeping only lowest-order terms in ϵ gives the linear stability equations

$$\lambda\tilde{\boldsymbol{u}} = -(\tilde{\boldsymbol{u}} \cdot \nabla)\boldsymbol{u}_b - (\boldsymbol{u}_b \cdot \nabla)\tilde{\boldsymbol{u}} - \nabla\tilde{p} + \frac{1}{Re}\boldsymbol{\nabla}^2\tilde{\boldsymbol{u}}, \tag{4a}$$

$$\boldsymbol{\nabla} \cdot \tilde{\boldsymbol{u}} = 0, \tag{4b}$$

where $\lambda = \sigma + i2\pi f$ is a (temporal) eigenvalue. Equations (4) are numerically solved using the same space-time discretisation as for the simulations of eqs. (1). An Arnoldi method is used to find the leading eigenvalues λ (those with largest growth rate σ) and corresponding 2D eigenmodes $\tilde{\boldsymbol{u}}$ [6]. Eigenvalues with positive σ correspond to unstable $\boldsymbol{u}_b$.

The thin curve in fig. 2 shows leading eigenvalues of the base flow. The onset of oscillation corresponds to a Hopf bifurcation in which the growth rate σ crosses zero at Re_c (by definition) with eigenfrequency f. The Strouhal number and eigenfrequency agree at the bifurcation, as they must at a supercritical bifurcation. However, past the bifurcation the frequencies diverge rapidly with Re. The eigenfrequency of $\boldsymbol{u}_b$ increases only slightly and then falls for Re above about 67. On the other hand, St increases rapidly following the bifurcation. This leads to the fact that for the cylinder wake the eigenvalues of the base flow are not predictive for the shedding frequency except very close to onset. It is in large part because the base flow eigenvalues fail to predict St-Re relationship that this relationship is difficult to explain.

Mean flows. – While the linear analysis of the base flow fails to capture the frequency of nonlinear vortex shedding, linear analysis of the mean flow provides an extremely good match, as we now address. For any T-periodic flow, $\boldsymbol{u}(x, y, t + T) = \boldsymbol{u}(x, y, t)$, the mean flow can be defined as $\bar{\boldsymbol{u}}(x, y) \equiv \langle \boldsymbol{u}(x, y, t)\rangle_T$. It is helpful to consider the decomposition of the flow into mean and fluctuating fields, $\boldsymbol{u}(x, y, t) = \bar{\boldsymbol{u}}(x, y) + \boldsymbol{u}'(x, y, t)$. Then $\bar{\boldsymbol{u}}$ obeys the time-averaged

Navier-Stokes equations

$$0 = -(\bar{\boldsymbol{u}} \cdot \nabla)\bar{\boldsymbol{u}} - \nabla\bar{p} + \frac{1}{Re}\boldsymbol{\nabla}^2\bar{\boldsymbol{u}} + \boldsymbol{F}, \tag{5a}$$

$$\nabla \cdot \bar{\boldsymbol{u}} = 0, \tag{5b}$$

where

$$\boldsymbol{F} = \boldsymbol{F}(x,y) \equiv -\left\langle (\boldsymbol{u}'(x,y,t)\cdot\nabla)\boldsymbol{u}'(x,y,t)\right\rangle_T$$

can be viewed as a forcing term due to Reynolds stresses generated by the fluctuating field.

From eqs. (5) we can understand the meaning of stability analysis of the mean flow. Consider the forced Navier-Stokes equations

$$\frac{\partial \boldsymbol{u}}{\partial t} + (\boldsymbol{u}\cdot\boldsymbol{\nabla})\boldsymbol{u} \;=\; -\nabla p + \frac{1}{Re}\boldsymbol{\nabla}^2\boldsymbol{u} + \boldsymbol{F}, \tag{6a}$$

$$\boldsymbol{\nabla}\cdot\boldsymbol{u} \;=\; 0. \tag{6b}$$

For a given Re take the forcing term $\boldsymbol{F}$ to be that given by the vortex shedding at that Re. Clearly $\bar{\boldsymbol{u}}$ will be a steady solution to eqs. (6). Then as for stability of the base flows, we can consider infinitesimal perturbations $\epsilon\tilde{\boldsymbol{u}}(x,y)\exp[\lambda t]$ to mean-flow solutions of the forced problem. Keeping only terms linear in ϵ gives the same linear equations as eqs. (4), but in terms of the mean flow $\bar{\boldsymbol{u}}$ rather than the base flow $\boldsymbol{u}_b$. The forcing term $\boldsymbol{F}$ does not appear since it is taken to be constant. Hence linear results must be properly interpreted as applying in the case where the Reynolds stresses are themselves unperturbed at order ϵ.

Figure 2 shows the leading eigenvalues from the linear analysis of the mean flow. The eigenfrequencies f agree almost exactly with St. Similar observations can been inferred from past studies of wake profiles [7, 8, 16, 18]. The analysis here is fully 2D and we also determine the growth rate σ of the 2D eigenmode. The growth rates in fig. 2(b) are almost exactly zero over the whole range of Re considered. *This implies that the mean flow, when viewed as a steady solution to the forced eqs.* (6)*, is marginally stable.* Both the eigenfrequency and growth rate observations are consistent with the model of Noack *et al.* [19].

While the mean-flow eigenfrequency is an extremely good predictor of the (nonlinear) Strouhal number, the mean flow is itself dictated by cumulative effects of vortex shedding over the cycle. The spatio-temporal symmetry of shedding suggests a method for approximating the mean flow from a single snapshot. Although this does not avoid the fundamental issue of requiring the vortex shedding solution, it eliminates the need to average over a shedding cycle and this could be important in experimental settings. Consider approximating the mean with two fields separated by half the period: $\bar{\boldsymbol{u}} \approx (\boldsymbol{u}(t_0) + \boldsymbol{u}(t_0 + T/2))/2$, where t_0 is some arbitrary reference time. From symmetry (3), $\boldsymbol{u}(t_0 + T/2)$ can be expressed in terms of $\boldsymbol{u}(t_0)$ and hence we obtain a two-point, or symmeterised, approximation to the mean flow

$$\boldsymbol{u}_h(x,y) \equiv \frac{1}{2}\left(u(x,y,t_0) + u(x,-y,t_0), v(x,y,t_0) - v(x,-y,t_0)\right).$$

This approximation is quite good. For example, fig. 1(e) shows $\boldsymbol{u}_h$ at $Re = 100$. In the near-wake region the difference between $\boldsymbol{u}_h$ and $\bar{\boldsymbol{u}}$ (fig. 1(d)) is small. The downstream part of $\boldsymbol{u}_h$ contains remnants of the vortex shedding and this part of approximation in particular depends on t_0. Figure 2 includes eigenvalues at three representative values of Re (60, 100, and 140) using $\boldsymbol{u}_h$ instead of $\boldsymbol{u}_b$ in eqs. (4). The eigenfrequencies f again agree almost exactly with St and they depend very weakly on the reference time t_0. The real part of the eigenvalues are centred about zero, though they show dependence on t_0 at larger Re.

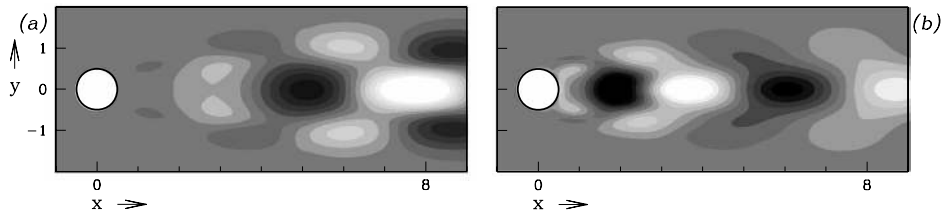

Fig. 3 – Vorticity of the leading eigenmode for (a) the base flow and (b) the mean flow at $Re = 100$.

The leading eigenmodes at $Re = 100$ for the base flow and the mean flow are shown in fig. 3. The modes are complex and are shown at one phase only. The streamwise spacing of vorticity maxima for the mean-flow eigenmode is almost identical to that of the vortex street in fig. 1(b). This is not the case for the base flow eigenmode.

Dynamics. – Figure 4 further illustrates the relationship between the mean flow, the base flow, and periodic oscillations at $Re = 100$. The time series, fig. 4(a), shows the value of v at a representative point $(x, y) = (2, 1)$. The phase portrait, fig. 4(b), shows this and v at the symmetrically related point $(2, -1)$ plotted so that reflection in y in the physical domain corresponds to reflection about the 45° line. The flow at $t = 0$ is perturbed slightly from $\boldsymbol{u}_b$. Oscillations develop which saturate in the periodic vortex shedding state. There is an increase in the oscillation frequency as the oscillation amplitude grows. This is the manifestation of the under-prediction of St by the stability analysis of $\boldsymbol{u}_b$. The oscillations do not develop symmetrically about $\boldsymbol{u}_b$, resulting in a change in the mean flow as the oscillations grow.

We would like to investigate the eigenvalues of the effective instantaneous mean flow as the oscillations grow. However, because the mean changes quite quickly on the time scale of the oscillations, extracting a precise instantaneous mean flow in the transient regime is problematic. A well-defined and meaningful family of steady flows is that given by solutions to eqs. (5) where $\boldsymbol{F}$ is replaced by $\alpha\boldsymbol{F}$. This gives $\boldsymbol{u}_b$ at $\alpha = 0$ and $\bar{\boldsymbol{u}}$ at $\alpha = 1$ and accounts for the growth of Reynolds stresses with oscillation amplitude. Figure 4(c) shows the relationship between growth rate and frequency as α varies between 0 and 1.25, extrapolating slightly beyond the mean flow at saturation. (Other families of flows, such as a linear interpolation

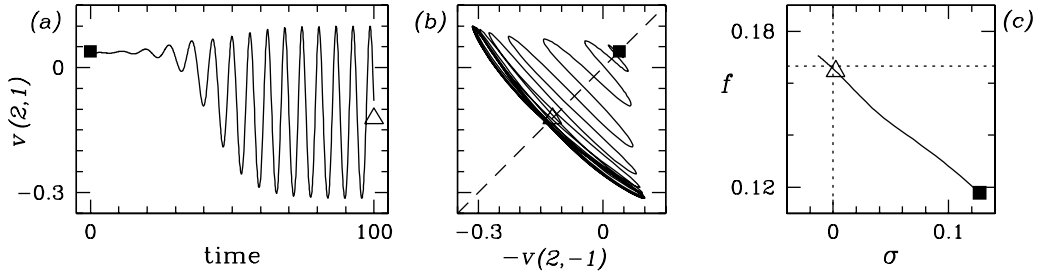

Fig. 4 – Relationship between the base flow $\boldsymbol{u}_b$ (denoted by squares) and the mean flow $\bar{\boldsymbol{u}}$ (denoted by triangles) at $Re = 100$. (a) Time series and (b) phase portrait showing the evolution from $\boldsymbol{u}_b$. The dashed line indicates the subspace of symmetric states. (c) Real and imaginary part of eigenvalues from stability analysis of solutions to eqs. (5) with $\alpha\boldsymbol{F}$, $0 \le \alpha \le 1.25$. Dashed lines indicate $\sigma = 0$ and $f = 0.167$, the Strouhal number at $Re = 100$.

$\boldsymbol{u} = \alpha\bar{\boldsymbol{u}} + (1-\alpha)\boldsymbol{u}_b$, give qualitatively similar results.) The interpretation is that, whatever the exact path taken by the instantaneous mean flow, the growth rate decreases and the eigenfrequency increases as oscillations grow. The oscillations saturate precisely when growth rate of the mean reaches zero, at which point the eigenfrequency is the Strouhal number.

Discussion. – Wesfreid *et al.* [12, 13, 15, 21] and Noack *et al.* [19, 20] have discussed at length the relationship between base flows and mean flows in the cylinder wake and related flows. In particular they have proposed that mean flow modification, through the formation of Reynolds stresses, is the mechanism for nonlinear saturation of oscillatory instability. The fully two-dimensional linear analysis presented here confirms a picture of nonlinear saturation in which the mean flow evolves to a state of marginal stability, at which point oscillations saturate in amplitude and have a frequency given by the eigenfrequency of the mean flow. Marginal stability of the mean flow is thus implicated in the selection of both amplitude and frequency in the oscillatory wake. It remains to be seen whether this result holds for other simple laminar flows.

* * *

I am grateful to J. E. Wesfreid, B. Thiria, B. Noack, G. Tadmor and L. Tuckerman for valuable discussions.

REFERENCES

[1] Bénard H., *C. R. Acad. Sci.*, **147** (1908) 839.
[2] von Kármán T., *Göttingen Nachr. Math. Phys. Kl.*, **12** (1912) 509.
[3] Jackson C. P., *J. Fluid Mech.*, **182** (1987) 23.
[4] Provansal M., Mathis C. and Boyer L., *J. Fluid Mech.*, **182** (1987) 1.
[5] Dusek J., LeGal P. and Fraunie P., *J. Fluid Mech.*, **264** (1994) 59.
[6] Barkley D. and Henderson R. D., *J. Fluid Mech.*, **322** (1996) 215.
[7] Mattingly G. E. and Criminale W. O., *J. Fluid Mech.*, **51** (1972) 233.
[8] Triantafyllou G. S., Triantafyllou M. S. and Chryssostomidis C., *J. Fluid Mech.*, **170** (1986) 461.
[9] Williamson C. H. K., *Phys. Fluids*, **31** (1988) 2742.
[10] Hammache M. and Gharib M., *J. Fluid Mech.*, **232** (1991) 567.
[11] Monkewitz P. A., Huerre P. and Chomaz J.-M., *J. Fluid Mech.*, **251** (1993) 1.
[12] Zielinska B. J. A. and Wesfreid J. E., *Phys. Fluids*, **7** (1995) 1418.
[13] Maurel A., Pagneux V. and Wesfreid J. E., *Europhys. Lett.*, **32** (1995) 217.
[14] Williamson C. H. K., *Annu. Rev. Fluid Mech.*, **28** (1996) 477.
[15] Zielinska B. J. A., Goujon-Durand S., Dusek J. and Wesfreid J. E., *Phys. Rev. Lett.*, **79** (1997) 3893.
[16] Hammond D. A. and Redekopp L. G., *J. Fluid Mech.*, **331** (1997) 231.
[17] Pier B. and Huerre P., *J. Fluid Mech.*, **435** (2001) 145.
[18] Pier B., *J. Fluid Mech.*, **458** (2002) 407.
[19] Noack B. R., Afanasiev K., Morzyński M., Tadmor G. and Thiele F., *J. Fluid Mech.*, **497** (2003) 335.
[20] Noack B. R., Tadmor G. and Morzyński M., in *Proceedings of the 2nd AIAA Flow Control Conference, Portland, Oregon, USA, 2004*, paper no. 2004-2408, *Conference Proceedings Series* (AIAA) 2006, Digital SKU: TMP.O.977 - MFCC04.
[21] Thiria B. and Wesfreid J. E., to be published in *J. Fluid Mech.*
[22] Stuart J. T., *J. Fluid Mech.*, **4** (1958) 1.
[23] Malkus W. V. R., *J. Fluid Mech.*, **1** (1956) 521.
[24] Henderson R. D. and Karniadakis G. E., *J. Comput. Phys.*, **122** (1995) 191.